International Journal of
INTELLIGENT SYSTEMS AND APPLICATIONS IN ENGINEERING
ISSN:2147-6799 www.ijisae.org Original Research Paper

Enhancing Passenger Vehicle Performance: A Study of CFD Technique and Machine Learning for Optimal Rear Spoiler Design and Lateral Stability

Raja Karthikeyan K.[1*], Arun Bhosale[2], Muhammad Sohaib Malik[3], Surrya Prakash Dillibabu[4], Vijaykumar Kisan Javanjal [5]

Submitted: 18/09/2023 **Revised**: 15/11/2023 **Accepted**: 28/11/2023

Abstract: In this study, the flow structure of a passenger automobile (the Volkswagen Vento) with rear spoilers is analyzed, and the most effective kind among numerous types is determined using a computational fluid dynamics (CFD) approach. CREO Parametric is used to create a 3D computer model of a sedan car, and ANSYS Fluent 17.2 is used to analyze forces operating on the element as a whole. The model is subjected to a pressure-based solver with k-ε turbulent model. This design is then utilized as the basis for further study. A spoiler is a component that protrudes from a car's back or tail and can be utilized to increase fuel economy. Although rear spoilers exist in a variety of shapes, they always serve the same purpose: by lowering drag, they enable more air to flow onto the body and reduce friction, maintaining a constant pressure zone beneath the vehicle. The vehicle's rear end spoiler redirects airflow, which aids in lowering flow separation. Because there is less flow separation, there is less drag, which leads to better fuel efficiency. It is researched how the wind will affect the car model with and without 5 types of spoilers. Drag, lift, and down forces are affected by the spoiler's varied shapes and angles. By employing the optimum specifications for the spoiler, the passenger car's vertical balance and fuel efficiency are enhanced. Furthermore, machine learning technique was used to predict the drag and lift force from the data acquired from this study. It was found that the machine learning module used was able to predict with an accuracy of 78% which indicates that the trained model is suitable for design consideration.

Keywords: *CFD, rear end spoiler, lateral stability, machine learning, aerodynamics*

1. Introduction

Aerodynamics is the study of how objects respond to air flow, especially when it comes into touch with a moving object [1], [2]. We may determine the various forces and moments operating on an object by understanding how air moves around it. Calculations based on position and time are used to calculate the properties, such as velocity, pressure, density, and temperature, of fluids. To calculate the aerodynamic efficiency, one can use mathematical analysis, empirical approximation, or wind tunnel testing. Its major objectives are to reduce noise emission, eliminate undesired lift forces, and reduce occurring drag and wind noise. Automotive aerodynamics are investigated through computer modelling and wind tunnel testing. The tunnel is sometimes equipped with a rolling thread mill like road to control the floor and to track the air flow to get more accurate results. This removes the boundary layer and enhances the performance of the high-speed object investigation. To reduce drag and increase fuel efficiency, engineers have created a number of techniques to channel air around moving objects by altering their shapes and smoothing their surfaces.

The rear spoiler is a component of an automobile that directs and modifies the airflow to lessen the aerodynamic drag of the vehicle.[3]–[7] They are frequently utilised on the wings or trailing edge of the body of racing cars. As the name implies, a spoiler is a deflector or tool used to divert pressure. Many automobiles, trucks, and SUVs include an air dam up front that lowers ground resistance[8]. Most modern cars have an attachment in the form of an upside-down wing called a rear backup spoiler[9]. The power of air pressure is mostly how it operates on automobiles. Although it started out as an attachment for racing vehicles, high-performance coupes are currently the main vehicle for which it is used. High speed cars' rear spoilers are specially engineered to increase stability at high speeds and decrease back lift on them [10]. In order to perform better, they can also increase the stability of passenger vehicles. [11], [12] Recent rear spoilers have a more practical purpose than purely aesthetic ones; they act more like fog lights to improve vision of the racer's potentially perilous blind region. [13]

A boundary layer forms when a fluid and a solid are moving relative to one another. When solid and fluid are moving in

[1] Panimalar Engineering College, Chennai, INDIA
[2] NBN Sinhgad Technical Institutes Campus, Pune, INDIA
[3] University of Illinois Urbana Champaign, Illinois, USA
[4]Vel Tech Rangarajan Dr. Sagunthala R&D Institute of Science and Technology, Chennai, INDIA
[5]Dr D Y Patil Institute of Technology Pimpri, Pune, INDIA
** Corresponding Author Email: k.rajakarthikeyan82@gmail.com*

relation to one another, a boundary layer is an imaginary layer of fluid that forms at a layer where the fluid's velocity is equal to 99% of free stream velocity. The flow speed is zero close to the body's wall and increases as it gets farther away. When there is relative motion between a fluid and a solid a boundary layer is formed. Skin friction occurs as the velocity at the surface of the air slows due to air viscosity. Because laminar flow has a smooth surface whereas turbulent flow has a rough surface, laminar and turbulent boundary layers acted differently. Aerodynamicists can make equations simpler by separating airflow into two halves, or Division of Flow. The Division of Flow is split into two groups, one outside the boundary layer and one inside it, where viscosity is a significant factor in drag. The boundary layer has a significant impact on both pressure and skin friction, which contributes significantly to aerodynamic drag. The vehicle's effective thickness is increased by the boundary layer, expanding the area where pressure drag occurs. Air molecules collide with the surface as the vehicle moves through the air, causing skin friction and a layer of turbulence[8]. A greater amount of skin friction is produced between them the more turbulent the fluid-and-skin interaction is.

The separation of the fluid flow occurs at certain spots where the change in velocity is blocked and the fluid begins to flow in the opposite direction as it passes over the surface of the vehicle. Typically occurring in the vehicle's rear, this phenomenon depends heavily on pressure distribution and is driven by the flow's outer layer. This alters the flow's behaviour at the back of the car, which has an impact on the flow field surrounding it. [15]. When a fluid flow separates from the surface of an item, flow separation takes place. An obstruction in the flow can increase drag in aerodynamics, especially pressure-induced drag, which depends on the air pressure difference between an object's front and back surfaces as they move through the air. [16,17] It has been demonstrated that flow separation causes a larger wake, which might hinder pressure recovery, which is negative. To prevent improper flow separation, the airflow transitions from the top to the rear window must be smoothed down. The lack of separation may also increase drag. The aerodynamics will operate better if the flows are in clean air (laminar flow). The boundary layer thickness can be decreased by improving the car's aerodynamics, preventing the worst flow separations**.**

A vehicle experiences a number of forces acting in different directions when it is moving quickly. Rolling resistance, drag, lift, and gravity are the four forces at work on the car, as shown in the free body diagram below. The total of the many forces preventing the vehicle from moving forward, such as weight, gravity, inertia, and air drag, is known as rolling resistance. In most modern cars, rolling resistance accounts for 3–11% of the energy consumed. Many people aren't aware of this, but lowering the vehicle's rolling resistance can result in significant fuel savings. [14]

The spoiler is an aerodynamic component of automobiles that "spoils" negative air movements, which are typically focused on drag. In order to manage airflow over an automobile, air dams are spoilers that are mounted on the front of the car[3, [4,] [13], [18]. By reducing air movement under the car, they also aid in lowering aerodynamic lift and drag. Although high-performance race cars and sports cars tend to have spoilers, passenger cars are starting to get them more frequently. Although spoilers are frequently used for styling, their aerodynamic effects are frequently negligible or even negative. Wings, front spoilers, lip spoilers, and pedestal spoilers are the many varieties. [11] This numerical research along with machine learning demonstrates that changes to the external design of the automobile body may be able to improve the aerodynamic performance of the vehicle and the usage of right spoiler to enhance the stability of the vehicle at higher speed. There is better cornering force when the vehicle stability increases this can be achieved with the help of the inclusion of the spoiler as many accidents occur during turning at high speeds.

2. Methodology

2.1. Data set

For the analysis, a 3D sedan automobile model is employed, and the car's rear end has spoilers fixed to it. The car model's size and design are displayed below [15].

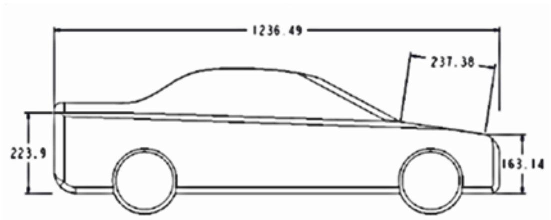

Fig. 1. - A side view of a typical sedan type with measurements

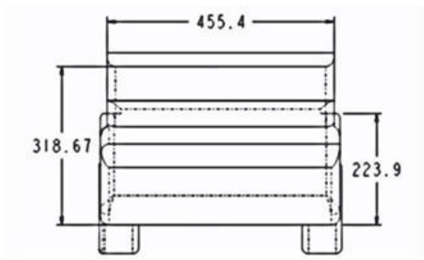

Fig 2- A rear view of a typical sedan type with measurements

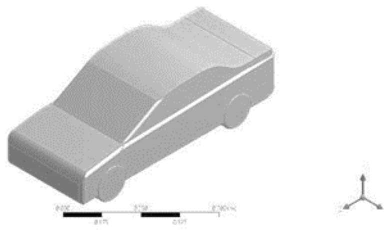

Fig 3 3D model of the sedan class model created using Solid works software and imported to Ansys

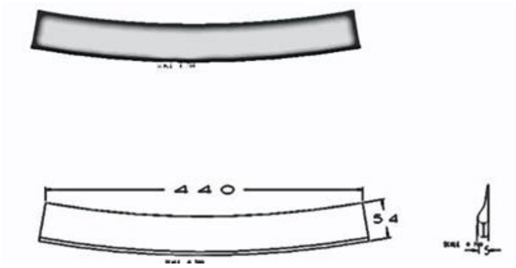

Fig 4 – SP1- A lip spoiler fitted to the vehicle's rear end

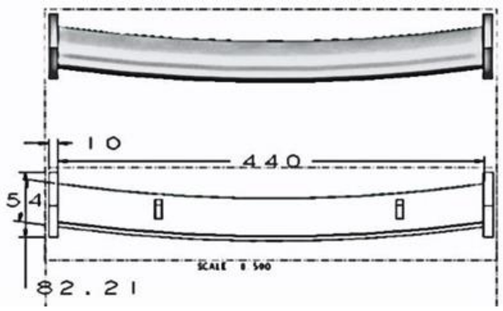

Fig 5 – SP2 - A single-bladed pedestal spoiler to change the airflow

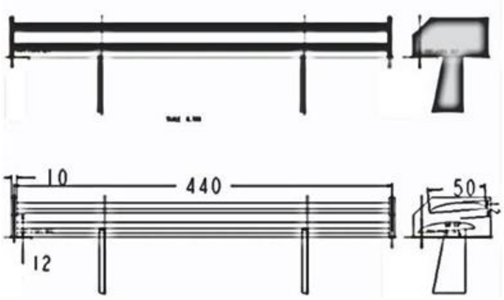

Fig 6 – SP3 - A pedestal spoiler with two blades, the higher blade located in the rear and the lower blade located in the front.

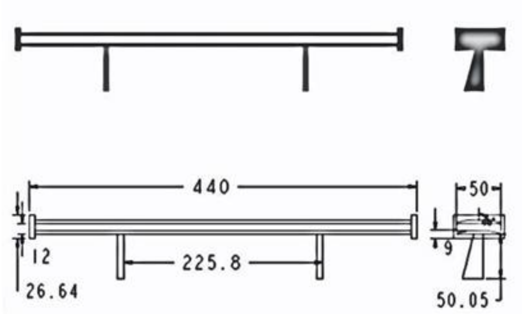

Fig 7 SP4 - A pedestal spoiler with two parallel, stacked blades, one above the other

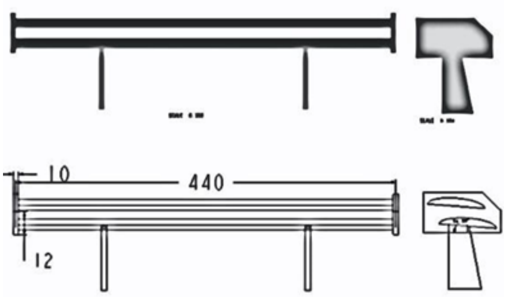

Fig 8 – SP5 - A pedestal spoiler with two blades, the top blade located up front and the bottom blade located down rear.

The methodology used has been explained in the flow chart given in Fig 9. It involves the Initialization, Solution control where solutions are being monitored by importing the model through .stp file. Meshing is carried out and the CFD calculation is done and the convergence of the different spoilers is checked for 100 iterations. If the results are satisfactory then the simulation is stopped or else the parameters are modified in the form of rearranging the meshing and the simulation is run again for better results. These steps are repeated until satisfactory results are attained.

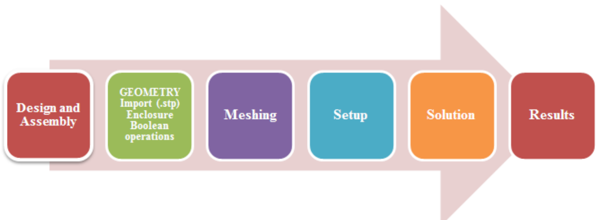

Fig 9. The methodology followed to check convergence in the various spoiler designs

2.2. Machine learning integration

2.2.1: Incorporating Machine Learning:

Machine learning methods are included into our study to better foretell and improve the vehicle's aerodynamic performance with and without a variety of different sorts of rear spoilers. We use machine learning algorithms to forecast aerodynamic performance metrics including drag, lift, down force, and efficiency.

The use of machine learning to the investigation of rear spoiler aerodynamics in passenger vehicles is a major step forward in that industry. By using this data, researchers will be able to better forecast complicated aerodynamic interactions, which will lead to more optimal designs for rear spoilers. Here, we'll discuss the ramifications of using machine learning in this study in further detail.

2.2.1.1 Training Data Collection:

A strong dataset is necessary for successful machine learning applications. The dataset used in this study is the result of extensive computational fluid dynamics simulations of several rear spoiler designs. The dataset is rather large, with thousands of data points representing various rear spoiler configurations for the vehicle. The specifications of the rear spoilers' design are included in this set of data as well as information on airflow patterns, pressure distributions, drag, lift, and down force values. Real-world variables like weather and traffic are reflected in the data as well.

2.2.1.2 Feature Engineering:

Feature engineering is used once a dataset has been established. Input features (parameters linked to rear spoiler design and vehicle characteristics) and output features (aerodynamic performance measurements) are selected and transformed as needed. To guarantee that the machine learning models have all the data they need to generate reliable predictions, feature engineering is an essential process. For instance, the aerodynamic forces are heavily influenced by the angle, form, and proportions of the rear spoilers, in addition to the car's speed. External impacts may be accounted for by adding variables such as vehicle weight and road conditions.

2.2.1.3 Choice of Machine Learning Models:

The integration relies heavily on the choice of machine learning models. Various models, such as regression analyses, neural networks, decision trees, and others, may be used. Regression models and deep neural networks are both taken into account in this study. For first screening, we employ regression models since they are fast, easy to understand, and can provide rough estimations of the rear spoiler's performance. However, neural networks are preferred because of their capacity to detect subtle, non-linear patterns in the data.

2.2.1.4 Model Training:

In the training phase, the selected machine learning models are fed the dataset. The models are tweaked and fine-tuned so that we may discover the connections between the parameters of the spoiler's design and the consequent aerodynamic properties. Internal parameters are refined in an iterative process to reduce the discrepancy between predicted and observed CFD data in the training set. This procedure is repeated until the models can reliably predict new data.

2.2.2: Rear Spoilers and their Impact:

Rear spoilers are standard equipment on modern automobiles, and its primary function is to increase efficiency by decreasing air resistance. Different types of spoilers have different purposes, but they always increase airflow over the vehicle, which decreases drag and keeps the pressure zone under the car stable. Rear spoilers prevent air from separating into separate streams by rerouting it. Drag is decreased as a consequence of this lessening of flow separation, and as a result, fuel economy is improved.

2.2.3: Machine Learning Incorporation:

Training machine learning models using CFD data helps researchers understand the intricate interplay between spoiler geometry, vehicle dynamics, and aerodynamic forces. Drag, lift, and down force, among others, may be predicted using these models of various spoiler configurations.

2.3. Design Consideration

Solidworks software was used to create a conventional car model, which was then imported into Ansys for analysis[13], [19], [20]. The position of the spoiler plays an important role as any slight difference will result in additional forces on the body. The position of the spoiler was chosen as per the standards prescribed. The different types of spoilers were chosen based on the combination of latest spoilers available in the market. Pedestal and Lip are the most commonly used ones in which varieties are available to enhance the aesthetics. Keeping in mind the aesthetics and efficiency of the car, the following models were chosen for study. The base model dimensions of the car has been shown in Fig 1 and Fig 2. Fig 3 shows the full shape of the car taken for this study. The length, height and width are 1236.49 x 318.67 x 455.4mm respectively

The analysis was done after the numerous spoilers were connected on the back end. The first model, SP0, does not have a spoiler and is used to study the effects of lift, drag, and turbulence. Regarding the second model, the SP1 is a lip spoiler as in Fig 4. The third spoiler, SP2, is an air-diversion pedestal spoiler with just one blade as in Fig 5. The fourth spoiler, SP3, is a pedestal spoiler with two blades that are positioned with the upper blade in the back and the lower blade in the front as in Fig 6. The fifth spoiler, SP4, is a pedestal spoiler with two parallel blades positioned one below the other as in Fig 7. The sixth spoiler, code-named SP5, is a pedestal spoiler with two blades, with the top blade being in the front and the bottom blade being in the back as in Fig 8. All models are investigated within a wind tunnel setup using the solver parameters provided in the table.

The kinematic eddy turbulent viscosity transfer equation is solved using the Spalart-Allmaras model, which is a one-problem model. [21]. The Spalart-Allmaras model has been demonstrated to yield good results for boundary layers with unfavourable pressure gradients. It was developed primarily for aerodynamic applications involving wall-bounded flows. [22] –[24] The car model with various types of spoilers is analysed using the Spalart-Allmaras turbulence model, which was created specifically for aerodynamic flows. [25]

2.4. Grid size test and validation

The meshing was done using coarse, medium and fine meshing options and the grid independency test was done. The quality of mesh generated has a direct influence on the model which are subjected high speed and hence the grid independency involving the various types of grains are determined. The number of elements generated and the velocity obtained at the outlet has been tabulated. As per richardson interpolation theory, factor greater than 1.3 is preferred as the mesh refinement ratio. The number of elements was getting higher as the grain size was made from coarse to fine. The output velocity was found to be getting more accurate as the grain size was increased. The refinement ratio between fine mesh and medium mesh is 1.85 and the refinement ratio between medium mesh and coarse mesh is 1.93. This proves that the generated mesh is in excellent condition and the results prove the same.

Table 1 – Grid Independency

	No. of Elements	*Velocity (m/s)*
Coarse	354689	42.25689
Medium	684578	42.26745
Fine	1268795	42.32456

2.5. Virtual Wind Tunnel Setup

A 3D CAD model that replicates a physical wind tunnel is enclosed virtually[26]. Since we are more interested in the back side of the vehicle, where the turbulence phenomenon occurs[21],[27],[28], greater space has been allowed on the rear side of the vehicle model to capture the flow behaviour predominantly behind the car[29]-[31]. The entrance, exit, and walls on each of the six sides of the virtual wind tunnel have been specified using the face selection option (enclosure). This enables the numerical solver in ANSYS FLUENT to recognise these faces and automatically apply the necessary boundary conditions. The wind tunnel setup are as follows length was set as 7000mm, height was 1500mm and the width was taken as 500mm.

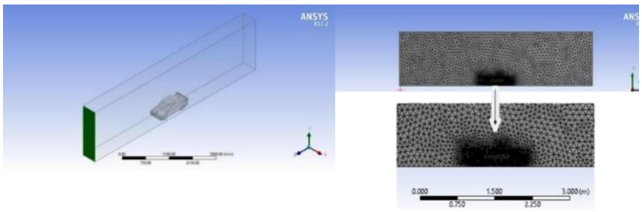

Fig 10 – View of a wind tunnel and meshed model element in symmetry

The geometry involved in the problem is discretely represented by meshing as shown in Fig 10. In order to estimate the equations and analyse the model, it divides space into elements (or cells or zones). For more precise results, the produced mesh has to be fine and smooth. The face and texture sizes are thus less than they would otherwise be compared to the default values. The Meshing was done using the inbuilt mesh tool in the Ansys Fluent software. Table 2 shows the mesh settings in which the minimum size was 0.00938m, the smoothing factor was kept to high to obtain a smooth flow over the surface. The other details have been mentioned appropriately. The solver settings have been tabulated in Table 3. All of these parameters are intended to produce a convergent, stable, and consistent numerical system. Here, stability is the characteristic that occurs when mistakes brought on by little changes in a numerical approach stay within bounds.

Table 2 –Mesh Settings

S No	*Meshing characteristics*	*Values*
1	Size function	Curvature
2	Relevance center	Coarse
3	Smoothing	High
4	Transition	Slow
5	Curvature normal angle	36 degrees
6	Minimum size	9.388e-3 m
7	Maximum face size	0.1m
8	Maximum texture size	0.1m
9	Growth rate	1.2
10	Nodes and elements in the body	Depends on the area of the mesh

Table 3 – Solver Settings

S	Parameters	Description
1	Type	Pressure- based
2	Velocity formulation	Absolute
3	Time	Steady
4	Models	Viscous - Spallart Allmaras Equation Fluid-air
5	Materials	Density = 1.225kg/m^3 Viscosity = 1.789e-5kg/m.s
6	Boundary Conditions	Inlet velocity = 35m/s Turbulent viscosity ratio = 10
7	Reference values	Area = 0.176m2
8	Initialization Methods	Hybrid initialization
9	No.of Iterations	100
10	Report Definitions	Drag force vector (x, y, z) = (0 ,0, -1) Lift force vector (x, y, z) = (0, 1, 0)

3. Result and Discussion

Using Ansys Fluent, the six models were put through a wind tunnel analysis, which produced data like velocity distribution, pressure distribution, drag and lift[12]. When comparing the velocity distribution graphs of the different spoiler types, it was discovered that SP2 and SP5 had less turbulence. It was discovered that SP3 had higher turbulence, which increases drag and reduces efficiency. The down force in SP2 and SP3 was found to be excessive when comparing the pressure distribution graphs of the various spoiler variants, which results in less lift. The higher pressure distribution at the back of the automobile, where air meets the spoiler blades, suggests that.

The car in SP0 has a drag coefficient of 0.512, whereas the SP4 and SP5 models created less drag than the latter (0.47). Because they are exactly related to one another, the drag force also decreases as the drag coefficient's value does. Therefore, utilizing the SP4 results in a 1.75 percent drag reduction, whereas using the SP5 results in an 8.2 percent drag reduction.

The car's lift coefficient in SP0 is -0.63. Because it represents the negative lift force in this situation, the lift coefficient is negative. Therefore, the lift force acting on the element is proportional to the lift coefficient value. The SP1 (-1.31) and SP3 regions have the least Cl (-1.18).

Although spoilers 1 and 3 have less lift, they are less effective because to their greater drag values. Thus, the SP5 is discovered to be the most effective spoiler model when the turbulence, drag, and lift of all the spoiler models are examined. The values of the lift and drag coefficients are 0.47 and -0.762, respectively. Comparing the data of the vehicle model SP0, the drag reduction is 8.2% and the lift reduction is 20.95%. In Fig 11 a), b) and c) swirls can be observed and the larger swirl can be seen in c) which indicates the recirculation zone behind the rear end of the vehicle. By comparing the swirls in Fig 11 b) and c) it seems to have a definite curl where in Fig 11 a) the swirl is disturbed and disoriented. In Fig 11 d) the outlet flow is totally disturbed and more like a zig zag pattern. In Fig 11 e) a slight turbulence can be observed at the rear baseline which is peculiar compared to all the other patterns. In Fig 11e) a small swirl can be seen which then gets converted into a streamline path later on. By comparing the recirculation zone in Fig b) and c) are definitely larger.

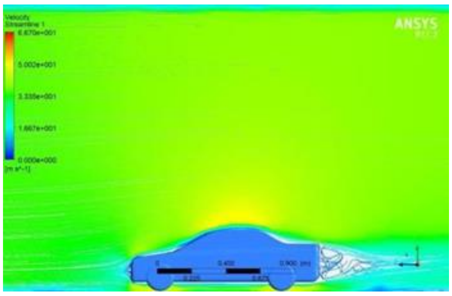

a)

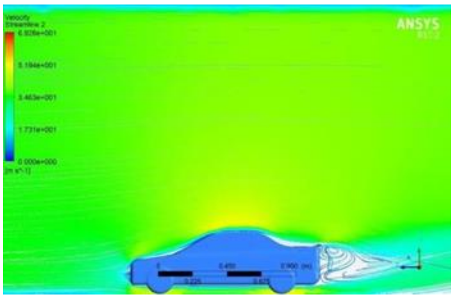

b)

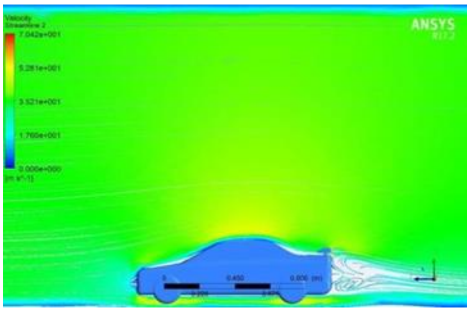

c)

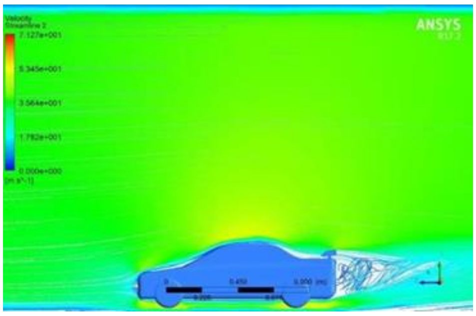

d)

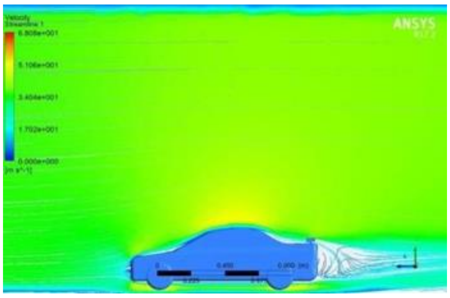

e)

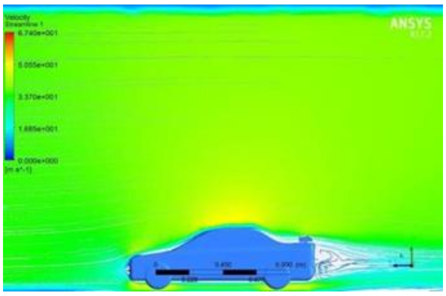

f)

Fig. 11. Distribution of different spoilers' velocities a) Without Spoiler b) Lip Spoiler c) Pedestal Spolier with Single Blade d) Pedestal with Two Blades — Front and Back e) Pedestal with Two Parallel Blades f) Pedestal with Two Blades — Front and Back

In pressure distribution streamlines in Fig 12 a) a smooth flow can be observed just after it leaves the tip of the read end but there can be seen two recirculation zones acting in opposite orientation. In Fig 12 b) and Fig 12 f) a similar recirculation zones can be observed but in Fig 12 f) it seems to be extend for a longer distance. The swirls are light and the zones are not much disturbed. Inconsistent zones can be observed in Fig 12 d) with a swirl at the farther end. Fig 12 c) and Fig 12 e) seems to have a smooth transition and the swirls are also not forming any curled up zones but it dilutes smoothly as the farther ends.

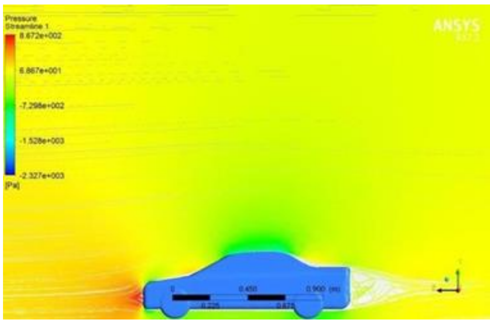

a)

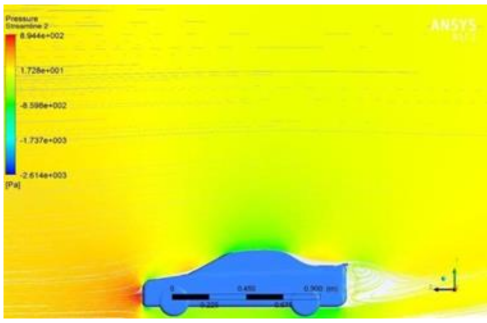

b)

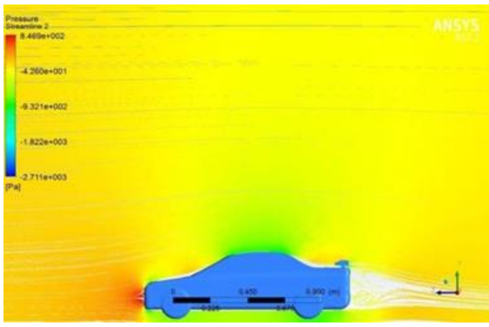

c)

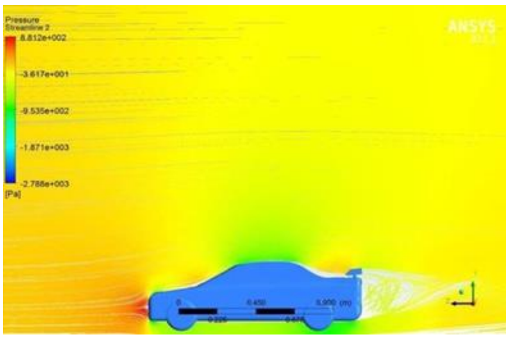

d)

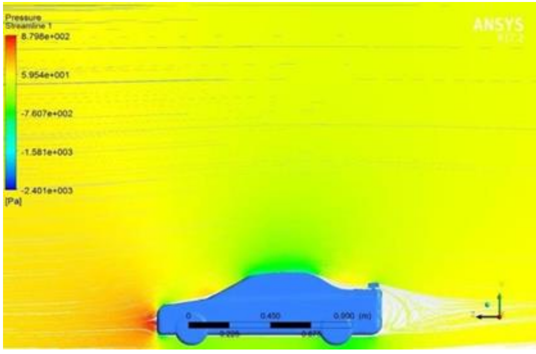

e)

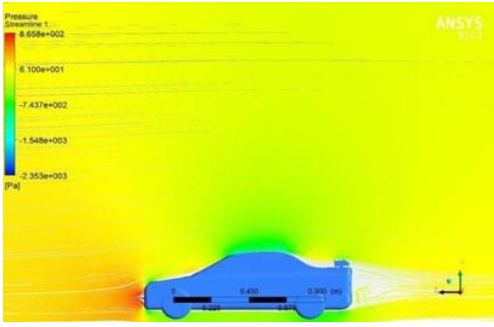

f)

Fig. 12. Different spoilers' pressure distribution a) Without Spoiler b) Lip Spoiler c) Pedestal Spoiler with Single Blade d) Pedestal with Two Blades — Front and Back e) Pedestal with Two Parallel Blades f) Pedestal with Two Blades — Front and Back

Table 3. Coefficients of Drag and Lift

Model	*Drag co-efficient* C_d	*Lift co-efficient* C_l
SP0	0.512	-0.63
SP1	0.625	-1.31
SP2	0.58	-1.11
SP3	0.67	-1.18
SP4	0.503	-0.87
SP5	0.47	-0.762

Table 4. List of Drag force and Lift force

Model	*Drag Force* F_d *(N)*	*Lift Force* F_l *(N)*
SP0	67.61	-83.19
SP1	82.53	-172.9
SP2	76.59	-146.58
SP3	88.47	-155.82
SP4	66.42	-114.88
SP5	62.06	-100.62

Table 3 and Table 4 lists out the values of the various values obtained from the simulation study for the drag coefficient, lift coefficient, drag force and lift force.

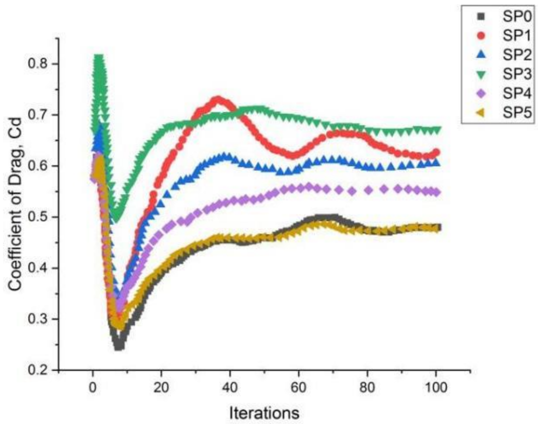

Fig 13 - Convergence diagram for the coefficient of drag (Cd) for the different spoiler types in comparison to the no-spoiler model

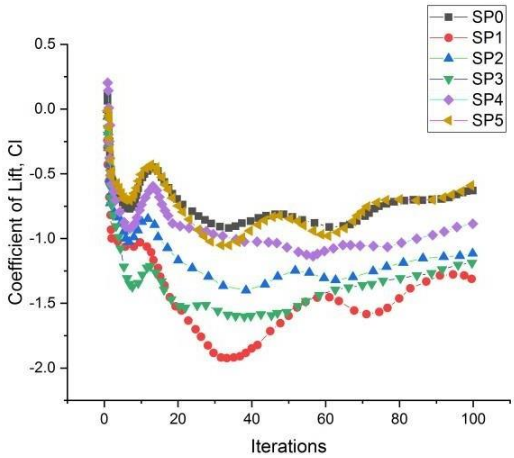

Fig 14 - Comparison of the various spoiler models' coefficients of lift and convergence with the model without a spoiler

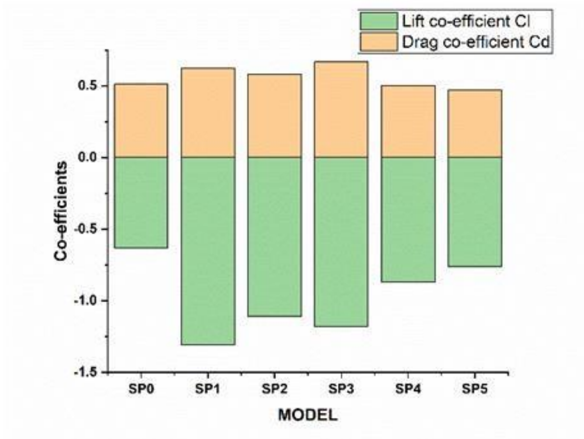

Fig 15 - Lift Coefficient Cl and Drag Coefficient Cd for all the spoilermodels considered

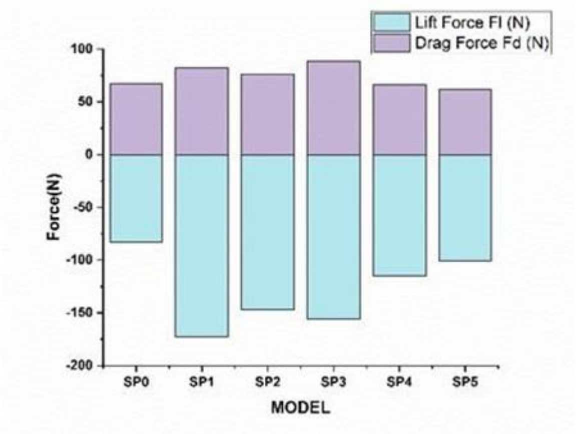

Fig 16 - Lift Force and Drag Force all the spoiler models considered

Figures 11 and 12 depict the velocity distribution of several spoiler models [9], [10], and [15]. In Fig 13 and Fig 14, the values of the turbulence created at various timelines have been displayed. The vehicle offers less resistance the less turbulence there is. Accordingly, a study was done to help us comprehend how the air flow model's impact on the spoiler was streamlined. The results fell within the expected ranges, and the matching numbers obtained indicated a gradual impact on the vehicle, which would therefore have an impact on its drag and lift. The red zones in the figures highlight the area that has an impact on the aerodynamics of the vehicle[3]. The maximum drag on the vehicle is indicated by the red zones in Fig. 12, and the strength varies depending on the surface of the vehicle. The air flow is smooth and streamlined on the surface model of the car in the yellow zones, which have the lowest drag. In Fig. 11, the light blue zones represent the smallest velocity impact on the vehicle, and the dark blue zones represent the maximum velocity effect. Using the Ansys programme, the pressure and velocity fluctuations were calculated from these diagrams.

The spoiler models SP5 are seen clearly [10], [12],[30],[32] in the convergence diagram of the coefficient of drag Cd Fig 13 as closely trailing the SP0 model. Due to the pedestal blades in the rear and front of the SP3 model, which cause turbulence in the medium, the SP3 model appears to be slightly taller. The midpoints of the iterations exhibit an additional coefficient of drag for the SP2 and SP4 models. Due to the lip spoiler model, the SP1 model exhibits waves during iteration. The outcome confirms that the spoiler's characteristics have an effect on the drag coefficient since it is located at the rear ends, where the medium's turbulence production is greatest. The system vibrates as a result of the boundary layer separation. Convergence diagram of Coefficient of Lift Cl Fig. 14 also shows the same characteristics. As can be observed, SP1 has a pattern that increases abruptly in the middle and then goes with the flow in the region of separation where the SPO and SP5 follow a more or less similar pattern. Due to the differences in model structures and blade positions in the spoilers, it can be seen that the other models in Cl are following a decremented format.

Separate calculations for the lift coefficient and drag coefficient resulted in results displayed in Fig 15. It demonstrates that SP3 has the highest drag coefficient, followed by SP1. The SP5 model had the least drag, which was less than the variant without a spoiler. For SP1 and SP3, the left coefficients were at their highest and lowest, respectively. The exact opposite relationship between drag and lift is demonstrated by the inversion of the drag coefficient. In Fig 16, the lift force and drag force are calculated and plotted. The SP3 and SP1 appear to have the highest drag, whereas the SP5 appears to have the lowest drag. The Lift force was greatest in SP1 and SP5, then SP5, and then SP1. This demonstrates that the drag and lift parameters unquestionably affect the surface design of the spoilers, with SP1 and SP3 having higher lift and drag than SP5.

3.1. Machine Learning Module

The data points obtained were generalized to form an individual drag force and lift force curves. The data points of these curves were subjected to polynomial regression using machine learning[33]. The data was split into 80% for training set and remaining 20% is used for testing set. After the training of model is completed, the model was evaluated using the testing set with the appropriate metrics. The most commonly used metric is the R squared value in which the R2 value of 0.92 is obtained for drag force curve as shown in Fig 17 and R2 value of 0.94 is obtained for lift curve as shown in Fig 18.

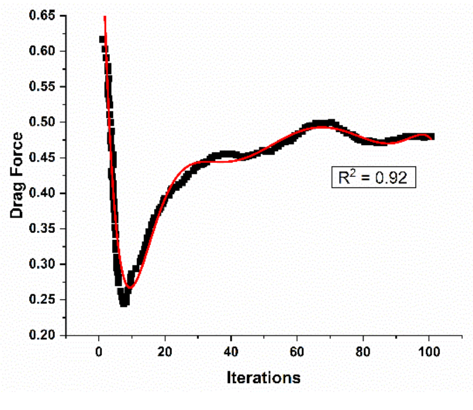

Fig 17. Polynomial regression applied to the generic drag force data points

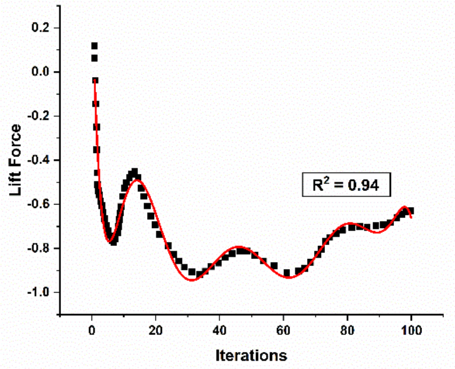

Fig 18. Polynomial regression applied to the generic lift force data points

The sensitivity of the model is in the close range and when a new value was given as input value the model was able to predict the desired output value with an accuracy of 78%. Thus this machine learning model is a useful technique for modeling complex relationships in data when a simple linear relationship isn't sufficient. It allows you to capture more nuanced patterns, making it a valuable tool in regression analysis.

Streamlined Predictive Analysis, important to this study is the use of machine learning algorithms to forecast the aerodynamic performance of various types of rear spoiler. These models allow engineers to avoid costly and time-consuming simulations for each design iteration by being trained on a complete dataset produced from extensive CFD simulations. The time it takes to fully evaluate how changes in form, angle, and other factors affect drag, lift, and downforce is reduced because to the impact of streamlining. Machine learning doesn't just stop at predictions; it offers valuable insights into the relative importance of design parameters. Engineers gain an understanding of which factors have the most significant impact on aerodynamic forces, contributing to informed decision-making. This insight empowers a deeper comprehension of the intricate relationships between design elements and aerodynamic performance, ultimately leading to more effective design choices.

Machine learning's incorporation into the optimization process ushers in a cycle of trial and error. Machine learning models may be retrained and fine-tuned to improve their forecast accuracy as new data becomes available or as the design process advances. This ongoing development helps to stimulate creativity and flexibility in the ever-evolving automobile industry by keeping rear spoiler designs at the cutting edge of aerodynamic efficiency.

Machine learning not only improves productivity in terms of its prediction and optimization abilities, but also in terms of the economy of both time and money. It shortens the design cycle by reducing the requirement for complex computational fluid dynamics (CFD) calculations and rigorous physical testing. As a result of this efficiency, manufacturers may lower their prices and provide customers with more affordable options. There are major ecological and monetary consequences of using machine learning in research. Reduced fuel consumption thanks to an optimized rear spoiler design is consistent with global sustainability goals since it results in less greenhouse gas emissions and a smaller environmental imprint. Manufacturers and consumers alike may reap the rewards of machine learning's efficiency gains throughout the design and engineering stages.

4. Conclusion

The goal of this study was to choose the most aerodynamic spoiler design for commercial cars. The different designs show that spoilers do affect moving vehicles, and because they are near the rear of the vehicle, the turbulence they generate must be appropriately channeled or it will have a negative impact on the vehicle. The spoilers do significantly alter this belief.

Comparing the velocity distribution diagrams of the various spoiler models, the turbulence was found to be less in spoiler models SP2 and SP5. The turbulence was found to be more in SP3 which causes more drag and so it becomes less efficient. Comparing the pressure distribution diagrams of the various spoiler models, the downforce was found to be high in spoiler models SP2 and SP3 and so the lift is reduced. It is inferred from the increased pressure distribution at rear portion of the car where the air hits the spoiler blades. The drag coefficient of the vehicle without the spoiler SP0 is 0.512 and the models which produced lesser drag than the later are SP4 (0.503) and SP5 (0.47). As the value of drag coefficient reduces, the drag force also reduces because it is directly proportional to each other. So the drag reduction using the SP4 is 1.75% and the drag reduction using the SP5 is 8.2%.

The lift coefficient of the vehicle without the spoiler SP0 is -0.63. Here the lift coefficient is negative because it represents the negative lift force. So, lower the value of the lift coefficient, lesser is the lift force acting on the element. The least Cl is found to be in SP1 (-1.31) and SP3 (-1.18). Although the lift is reduced in SP1 and SP3, their drag values are higher which makes them less efficient. So, examining the turbulence, drag and lift of all the spoiler models, the SP5 is found to be the most efficient one. The drag and lift coefficient values are 0.47 and -0.762 respectively. The drag reduction is 8.2% and the lift reduction is 20.95% comparing with the values of the vehicle model without the spoiler. This study highlights the potential of CFD techniques along with machine learning model in designing efficient rear-end spoilers for passenger vehicles, with a specific focus on lateral stability. Our findings have practical implications for the automotive industry, as they can contribute to the development of safer and more stable vehicles. Overall, this investigation represents a significant step towards achieving safer and more efficient passenger vehicles on the road.

Conflicts of interest

The authors declare no conflicts of interest.

References

[1] S. Hetawal, M. Gophane, B. K. Ajay, and Y. Mukkamala, "Aerodynamic study of formula SAE car," Procedia Eng., vol. 97, pp. 1198–1207, 2014, doi: 10.1016/j.proeng.2014.12.398.

[2] X. Hu, R. Zhang, J. Ye, X. Yan, and Z. Zhao, "Influence of different diffuser angle on Sedan's aerodynamic characteristics," Phys. Procedia, vol. 22, pp. 239–245, 2011, doi: 10.1016/j.phpro.2011.11.038.

[3] X. Hu and E. T. T. Wong, "A Numerical Study On Rear-spoiler Of Passenger Vehicle," pp. 636–641, 2011.

[4] V. S. Modelling, "Aerodynamic analysis of an active rear split spoiler for improving lateral stability of high-speed vehicles Divya Teja Ayyagari and Yuping He *," vol. 12, 2017.

[5] C. V. K. B. Murugan, P. A. N. Ashik, and P. Raju, "CFD Analysis and Optimization of a Car Spoiler," vol. 5, no. 1, pp. 128–133, 2015.

[6] R. Chandra and M. Riyad, "CFD Analysis of Passenger Vehicleat Various Angle of Rear End Spoiler," Procedia Eng., vol. 194, pp. 160–165, 2017, doi: 10.1016/j.proeng.2017.08.130.

[7] M. Cakir, "CFD study on aerodynamic effects of a rear wing / spoiler on a passenger vehicle," 2012.

[8] A. R. Norwazan, A. J. Khalid, A. K. Zulkiffli, O. Nadia, and M. N. Fuad, "Experimental and Numerical Analysis of Lift and Drag Force of Sedan Car Spoiler," vol. 165, pp. 43–47, 2012, doi: 10.4028/www.scientific.net/AMM.165.43.

[9] C. S. Yuan, S. Mansor, and M. A. Abdullah, "Effect of Spoiler Angle on the Aerodynamic Performance of Hatchback Model," vol. 12, no. 22, pp. 12927–12933, 2017.

[10] M. M. Hudson and E. D. Raj, "Investigating the Effect of Rear Spoiler and Rear Diffuser on Aerodynamic Forces using CFD," vol. 3, no. 26, pp. 1–6, 2015.

[11] S. Cheng and S. Mansor, "Influence of spoiler on the aerodynamic performance of hatchback vehicle," vol. 01027, 2017.

[12] H. S. Hamut, R. S. El-emam, and I. Dincer, "Effects of rear spoilers on ground vehicle aerodynamic drag," pp. 627–642, 2014, doi: 10.1108/HFF-03-2012-0068.

[13] T. Ning, Y. Zhang, and L. Fu, "IOP Conference Series : Materials Science and Engineering Aerodynamics analysis of the car using Solidworks flow simulation with rear spoiler using CFD Aerodynamics analysis of the car using Solidworks flow simulation with rear spoiler using CFD," 2020, doi: 10.1088/1757- 899X/993/1/012002.

[14] M. Szudarek, "CFD Analysis of the Influence of the Front Wing Setup on a Time Attack Sports Car ' s Aerodynamics," 2021.

[15] D. Syafiq, B. Maji, and N. Mustaffa, "FMC CFD Analysis of Rear-Spoilers Effectiveness on Sedan Vehicle in Compliance with Malaysia National Speed Limit," vol. 3, no. 1, pp. 1–7, 2021.

[16] S. Bezavada, "Numerical simulation of air flow over a passenger car and the Influence of rear spoiler using CFD Numerical simulation of air flow over a passenger car and the Influence of rear spoiler using CFD," no. December 2012, 2019.

[17] V. N. Kumar, K. L. Narayan, L. N. V. N. Rao, Y. S. Ram, and V. N. Kumar, "Investigation of Drag and Lift Forces over the Profile of Car with Rearspoiler using CFD," vol. 1, no. 08, pp. 331–339, 2015, doi: 10.7439/ijasr.

[18] F. Frihdianto, N. Sriwardani, and I. Widiastuti, "ANALYSIS OF THE USE OF SPOILER ONE LEVEL AND TWO LEVELS IN CONDITIONS OF STEADY AGAINST THE DRAG AND LIFT COEFFICIENTS ON A SEDAN TYPE CAR BY USING CFD (COMPUTATIONAL FLUID DYNAMIC)," vol. 1, no. 2, pp. 58–64, 2018.

[19] A. Yadav, P. Rawal, and R. K. Mishra, "Modelling and simulation of aerodynamic performance of Vortex generators for hatch back type cars," pp. 131–136, 2018, doi: 10.21595/vp.2018.20399.

[20] E. Gunpinar, U. C. Coskun, M. Ozsipahi, and S. Gunpinar, "A Generative Design and Drag Coefficient Prediction System for Sedan Car Side Silhouettes based on Computational Fluid Dynamics," CAD Comput. Aided Des., vol. 111, pp. 65–79, 2019, doi: 10.1016/j.cad.2019.02.003.

[21] Y. Liu, L. Lu, L. Fang, and F. Gao, "Modification of Spalart – Allmaras model with consideration of turbulence energy backscatter using velocity helicity," Phys. Lett. A, vol. 375, no. 24, pp. 2377–2381, 2011, doi: 10.1016/j.physleta.2011.05.023.

[22] A. Bueno-orovio and F. Palacios, "Continuous Adjoint Approach for the Spalart – Allmaras Model in

Aerodynamic Optimization," vol. 50, no. 3, 2012, doi: 10.2514/1.J051307.

[23] G. H. Yoon, "Topology optimization for turbulent flow with Spalart-Allmaras model," Comput. Methods Appl. Mech. Engrg., 2016, doi: 10.1016/j.cma.2016.01.014.

[24] Y. Bao, D. Zhou, C. Huang, Q. Wu, and X. Chen, "Numerical prediction of aerodynamic characteristics of prismatic cylinder by finite element method with Spalart – Allmaras turbulence model," Comput. Struct., vol. 89, no. 3–4, pp. 325–338, 2011, doi: 10.1016/j.compstruc.2010.10.019.

[25] A. S. Zymaris, D. I. Papadimitriou, K. C. Giannakoglou, and C. Othmer, "Computers & Fluids Continuous adjoint approach to the Spalart – Allmaras turbulence model for incompressible flows," Comput. Fluids, vol. 38, no. 8, pp. 1528–1538, 2009, doi: 10.1016/j.compfluid.2008.12.006.

[26] T. Under and L. Reynolds, "Small-Scale Wind Turbine Testing in Wind Ac ce pt ed nu sc r ip t N ot py ed ite d Ac ce pt Ma r t N Co py ed d," no. c, 2015, doi: 10.1115/1.4030617.

[27] Z. Yang and M. Schenkel, "Assessment of Closed-Wall Wind Tunnel Blockage using CFD," vol. 2004, no. 724, 2018.

[28] W. Wang, P. Liu, Y. Tian, and Q. Qu, "Numerical study of the aerodynamic characteristics of high-lift droop nose with the deflection of fowler flap and spoiler," Aerosp. Sci. Technol., vol. 48, pp. 75–85, 2016, doi: 10.1016/j.ast.2015.10.024.

[29] "Particle Image Velocimetry in Aerodynamics : Technology and Applications in Wind Tunnels," vol. 2, pp.229–244, 2000.

[30] H. Snel, "Review of Aerodynamics for Wind Turbines," vol. 211, pp. 203–211, 2003, doi: 10.1002/we.97.

[31] C. H. Tsai, L. M. Fu, C. H. Tai, Y. L. Huang, and J. C. Leong, "Computational aero-acoustic analysis of a passenger car with a rear spoiler," Appl. Math. Model., vol. 33, no. 9, pp. 3661–3673, 2009, doi: 10.1016/j.apm.2008.12.004.

[32] L. Hanimann, L. Mangani, A. K. Dhillon, E. Abdellah, and B. Wang, "Rear-roof spoiler effect on the aerodynamic drag performance of a simplified hatchback model Rear-roof spoiler effect on the aerodynamic drag performance of a simplified hatchback model," 2017, doi: 10.1088/1742-6596/755/1/011001.

[33] Jacob, Sam Jacob, Markus Mrosek, Carsten Othmer, and Harald Köstler. "Deep learning for real-time aerodynamic evaluations of arbitrary vehicle shapes." arXiv preprint arXiv:2108.05798 (2021). https://doi.org/10.48550/arXiv.2108.05798